JCB Article

Processing by proprotein convertases is required for glypican-3 modulation of cell survival, Wnt signaling, and gastrulation movements

Bart De Cat,[1] Sin-Ya Muyldermans,[1] Christien Coomans,[1] Gisèle Degeest,[1] Bernadette Vanderschueren,[1] John Creemers,[2] Frédéric Biemar,[3] Bernard Peers,[3] and Guido David[1]

[1]Laboratory for Glycobiology and Developmental Genetics and [2]Laboratory for Molecular Oncology, Department of Human Genetics, University of Leuven and Flanders Interuniversity Institute for Biotechnology, B-3000 Leuven, Belgium
[3]Laboratoire de Biologie Moléculaire et de Génie Génétique, Université de Liège, B-4000 Liège, Belgium

Glypican (GPC)-3 inhibits cell proliferation and regulates cell survival during development. This action is demonstrated by GPC3 loss-of-function mutations in humans and mice. Here, we show that the GPC3 core protein is processed by a furinlike convertase. This processing is essential for GPC3 modulating Wnt signaling and cell survival in vitro and for supporting embryonic cell movements in zebrafish. The processed GPC3 core protein is necessary and sufficient for the cell-specific induction of apoptosis, but in vitro effects on canonical and noncanonical Wnt signaling additionally require substitution of the core protein with heparan sulfate. Wnt 5A physically associates only with processed GPC3, and only a form of GPC3 that can be processed by a convertase is able to rescue epiboly and convergence/extension movements in GPC3 morphant embryos. Our data imply that the Simpson–Golabi–Behmel syndrome may in part result from a loss of GPC3 controls on Wnt signaling, and suggest that this function requires the cooperation of both the protein and the heparan sulfate moieties of the proteoglycan.

Introduction

Loss-of-function mutations of *GPC3*, the gene that encodes glypican (GPC)-3, cause Simpson–Golabi–Behmel syndrome (SGBS) in humans. This X-linked syndrome is characterized by prenatal and postnatal overgrowth, visceral and skeletal anomalies, and an increased risk for the development of embryonal tumors (Pilia et al., 1996). The clinical features of these patients and the phenotypes of two independently generated *Gpc3* knockout mouse models (Cano-Gauci et al., 1999; Paine-Saunders et al., 2000) suggest that GPC3 inhibits cell proliferation and regulates cell survival during development, but the mechanisms involved remain unclear. Based on the phenotypic similarity of SGBS and the Beckwith–Wiedemann syndrome, it has been proposed that GPC3 might interfere with insulin-like growth factor (IGF) II signaling (Pilia et al., 1996), but crossbreeds of *Gpc3*−/− and *Igf*-deficient mouse strains suggest an IGF-independent overgrowth mechanism in the Gpc3 knockout mice (Chiao et al., 2002). More consistent is the genetic evidence in flies, mice, *Xenopus laevis*, and zebrafish that implicates GPCs in the regulation of Wingless/Wnt and Dpp/Bmp signaling, pathways that direct cell fates, migration, and proliferation during embryogenesis and in adult tissues (Jackson et al., 1997; Paine-Saunders et al., 2000; Baeg et al., 2001; Grisaru et al., 2001; Topczewski et al., 2001; Tsuda et al., 2001; Fujise et al., 2003; Ohkawara et al., 2003).

Only limited information is available on the molecular and cellular mechanisms that support this signaling function (Song and Filmus, 2002). GPCs are heparan sulfate proteoglycans (HSPGs) that are linked to the cell surface via glycosylphosphatidylinositol (GPI). As such, GPCs qualify as receptors or coreceptors for several heparin-binding proteins including morphogens, growth factors, adhesion, and matrix molecules; and they are potentially involved in shaping the concentration gradients and activity ranges of these molecules. Yet, the distinctive part of a GPC is its protein core. Six GPCs (GPC1–6) have been identified in vertebrates, two

Address correspondence to Guido David, Center for Human Genetics, Campus Gasthuisberg, Herestraat 49, B-3000 Leuven, Belgium. Tel.: 32-16-345863. Fax: 32-16-347166. email: guido.david@med.kuleuven.ac.be

Key words: glypican; Wnt; furin; epiboly; apoptosis

Abbreviations used in this paper: BFA, brefeldin A; CRD, cysteine-rich domain; GPC, glypican; GPI, glycosylphosphatidylinositol; hpf, hours post fertilization; HS, heparan sulfate; HSPG, heparan sulfate proteoglycan; JNK, c-Jun NH_2-terminal protein kinase; PC, proprotein convertase; SGBS, Simpson-Golabi-Behmel syndrome.

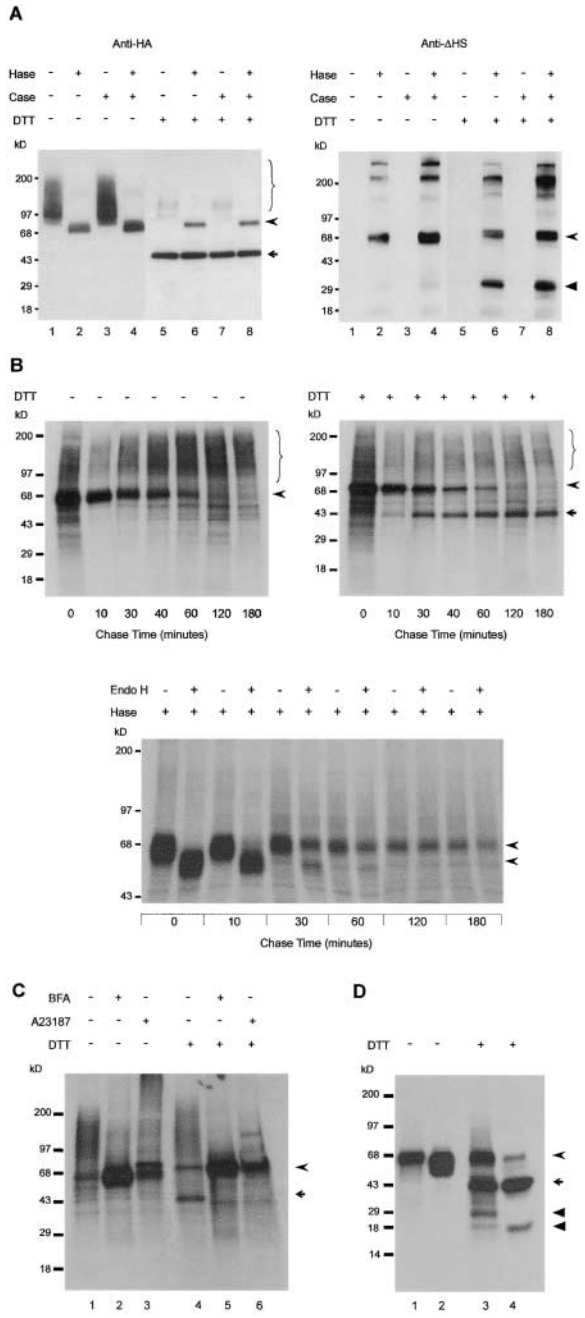

Figure 1. **Posttranslational modification of GPC3 in MDCK cells.** Total proteoglycan or GPC3 isolated from stable transfectant cells was treated with heparitinase (Hase), chondroitinase ABC (Case), or endoglycosidase H (Endo H) as indicated, and fractionated by SDS-PAGE under reducing (DTT) or nonreducing conditions. (A) Two-subunit structure of GPC3. Western blots of total proteoglycan extract, using rat anti-HA mAb 3F10 to detect GPC3, and anti-ΔHS mAb 3G10 to detect the desaturated uronates that are generated by heparitinase and that remain in association with the core proteins. (B) Time course of the GPC3 maturation. Cells were pulse labeled with [^{35}S]cysteine-methionine for 10 min and chased for the indicated time periods. GPC3 from cell lysates, isolated using anti-HA antibody, was detected by autoradiography. Unreduced (left) and reduced (right) non enzyme-treated samples (top), and reduced glycosidase-treated samples (bottom) reveal that the HS substitution, proteolytic processing, and Endo H–resistant N-glycosylation of GPC3 follow similar time courses. (C) Inhibition of GPC3 processing by blocking ER export or calcium depletion. Cells were incubated for 6 h with (+) or without (−) 30 μM BFA or 2 μM A23187, pulse-labeled for 10 min, and chased for 60 min. GPC3 immunopurified from cell lysate was detected by autoradiography. (D) Endoproteolytic processing of GPC3ΔHS. Labeled HA-GPC3ΔHS was immunoprecipitated from the cell lysate (lanes 1 and 3) and the conditioned medium (lanes 2 and 4). Braces show glycanated GPC3, curved arrowheads indicate the GPC3 core protein, arrows indicates the ∼40-kD NH_2-terminal (HA-tagged) α-subunit, and arrowheads indicate the COOH-terminal β subunit that is separated from the α-subunit by reduction. Numbers on the left represent molecular mass markers.

in *Drosophila melanogaster*, and one in *Caenorhabditis elegans*. All GPC core proteins have a similar domain structure, starting with a signal peptide, followed by a large globular cysteine-rich domain (CRD), a smaller stalk-like domain with the heparan sulfate (HS) attachment sites, and, finally, a signal sequence for GPI attachment. 14 cysteines, in concert with several additional amino acids that occur at invariant positions, compose a unique sequence motif that has been strictly conserved in all GPCs, suggesting some highly conserved specific function for the CRD. Recently, Chen and Lander (2001) have demonstrated that the CRD of GPC1 strongly influences the HS substitution of the core protein.

GPCs are constitutively shed from the surfaces of cultured cells, but it is not clear whether this involves phospholipase activities that cleave the GPI anchor and/or protease activities that cleave at the level of the stalk domain. It is also not known whether shedding represents a physiological process, and whether this might down-regulate these molecules or render their functions non-cell autonomous. Yet, membrane anchorage is required for GPC3 to induce cell lineage-specific apoptosis (Gonzalez et al., 1998). Here, we report that GPC3 is subjected to endoproteolytic processing. This processing is distinct from the shedding step because it occurs in the CRD. It generates two core protein subunits, designated as α and β, which remain in association with one another through disulfide bonding, and with the cell surface via the GPI-tail of the β subunit. This processing is mediated by members of the proprotein convertase (PC) family, and is essential for GPC3 to modulate Wnt signaling in cultured cells, to induce apoptosis in specific cell types via the activation of c-Jun NH_2-terminal protein kinase (JNK), and to support epiboly and convergence/extension movements in zebrafish gastrulae.

Results

Endoproteolytic processing of GPC3

To characterize GPC3, we introduced an HA epitope into the NH_2 terminus of the protein. In MDCK cells that stably expressed this construct, most of HA-GPC3 was converted into proteoglycan (Fig. 1 A, left, lane 1). After heparitinase digestion (with or without an additional chondroitinase ABC digestion), nonreduced GPC3 yielded a protein core of ∼65 kD (lanes 2 and 4). In contrast, under reducing conditions, we mainly detected a discrete ∼40 kD HA-tagged band (lane 5). Heparitinase and chondroitinase ABC treatments had no influence on the apparent molecular mass of this band (lanes 6–8). From this, we tentatively concluded that the protein core of GPC3 might consist of two disulfide-linked subunits,

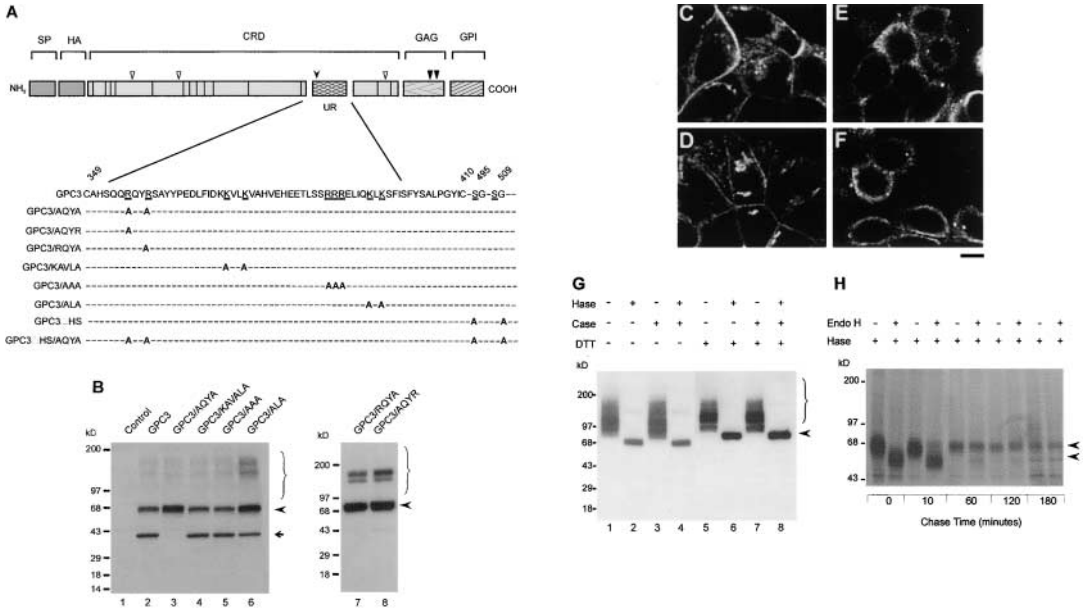

Figure 2. **Identification of the cleavage site in GPC3.** (A) Schematic representation of GPC3. The GPC3 domains are depicted as shaded boxes. Lines within the boxes denote cysteine residues of the CRD, as conserved in all glypicans (GPCs). Open arrowheads denote potential N-glycosylation sites; closed arrowheads indicate the positions of the HS attachment sites. The curved arrowhead indicates the position of the proteolytic cleavage site. This latter site occurs in a region of the CRD that shows low sequence similarity to corresponding regions in other GPCs. Amino acid substitutions, as indicated in bold, were introduced into this unconserved region (UR) and in the HS substitution domain (GAG), either alone or in combination. SP, signal peptide for membrane translocation; HA, hemagglutinin tag; CRD, cysteine-rich domain; GPI, signal peptide for glypiation. (B) Endoproteolytic processing of the GPC3 mutants. Whole extracts of CHO-K1 cells transiently transfected with a control vector, wild-type GPC3 or mutant forms of GPC3, were fractionated by SDS-PAGE under reducing conditions, and analyzed by Western blotting using rat anti-HA mAb 3F10. (C–F) Subcellular localization of GPC3 and GPC3/AQYA. Horizontal confocal sections of stable MDCK clones expressing GPC3 (top) or GPC3/AQYA (bottom), fixed and stained with rat anti-HA mAb 3F10, without (left) or after permeabilization (right). Bar, 10 μm. (G) Glycanation and endoproteolytic processing of GPC3/AQYA. Proteoglycan isolated from stably transfected MDCK cells was treated with the indicated enzymes, fractionated by SDS-PAGE under reducing and nonreducing conditions, and analyzed by Western blotting using rat anti-HA mAb 3F10. (H) Maturation of GPC3/AQYA. Stable transfectant MDCK cells were pulse labeled with [^{35}S]cysteine-methionine for 10 min and chased for the indicated time periods. Mutant GPC3, immunopurified from cell lysate, was treated with the indicated enzymes, fractionated by SDS-PAGE under reducing conditions, and detected by auroradiography. Braces show glycanated GPC3/AQYA; curved arrowheads indicate the GPC3/AQYA core protein. Numbers on the left represent molecular mass markers.

whereby the NH_2-terminal (α) subunit has a size of ~40 kD (HA-tagged fragment) and the COOH-terminal (β) subunit, with the sites for the attachment of the HS chains, has a size of ~30 kD. Consistently, after heparitinase digestion, such a β subunit could be detected with 3G10, an mAb specific for a neo-epitope that includes the Δ-glucuronate generated by the enzyme (Fig. 1 A, right, compare lanes 2 and 4 with 6 and 8). Shed GPC3 accumulating in the conditioned culture media of these cells was also an endoproteolytically processed HSPG (unpublished data).

The time course of the proteolytic maturation of GPC3 was analyzed by a series of pulse-labeling and chase experiments, and related to other posttranslational modifications of the protein. Proteolytic maturation, acquisition of endo H-resistance, and substitution with HS followed similar time courses (Fig. 1 B). Treatment with Brefeldin A (BFA) inhibited both the HS substitution and the proteolytic processing of GPC3 (Fig. 1 C), indicating the requirement for a post-ER compartment. Both posttranslational modifications were also inhibited by the calcium ionophore A23187 (Fig. 1 C), suggesting the involvement of calcium-dependent cisternal enzymes. Finally, an HS-deficient mutant (GPC3ΔHS), created by mutating the serines at the two potential HS attachment sites into alanines, was also normally processed in two subunits (Fig. 1 D). The α subunits from both the cell extract and the conditioned medium migrated as ~40 kD fragments. However, the β subunit from the cell extract migrated slightly more slowly than its counterpart from the conditioned medium (Fig. 1 D, compare lane 3 with lane 4). This suggests a second proteolytic event, potentially related to the shedding of GPC3 from the cell surface. Together, these data suggest a scheme whereby GPC3 is synthesized as a proprotein in the ER, where it is transferred to GPI and N-glycosylation is initiated. Then, it shuttles to the Golgi complex, where it is further N-glycosylated, O-glycanated, and processed into two subunits, and travels to the cell surface. Ultimately, a second proteolytic event separates the protein from the GPI anchor, and the protein is shed.

Endoproteolytic processing of GPC3 depends on a paired basic motif in the CRD

To identify the processing site, we mutated four potential protease-cleavage consensus sequences in GPC3. All of these sequences are located between Cys^{349} and Lys^{405}, potentially yielding an NH_2-terminal HA-tagged fragment of ~40 kD (Fig. 2 A). All mutants were tested by transient transfection in CHO-K1 cells. Processing was abolished in the GPC3/AQYA mutant, but unaffected in the three

other mutants (Fig. 2 B, lanes 2–6). To further identify $R^{355}QYR^{358}$ as the cleavage site and as a paired basic motif, we tested two additional mutants, GPC3/RQYA and GPC3/AQYR. Both mutants yielded only unprocessed forms of GPC3 (Fig. 2 B, lanes 7–8).

The repercussions of these mutations in terms of intracellular trafficking, proteolytic processing, and HS substitution were further analyzed in stably transfected MDCK cells. Both GPC3 and GPC3/AQYA accumulated at the cell surface (Fig. 2, C and D). Compilations of series of confocal images along the z axis revealed that both forms of GPC3 were accumulating over both the apical and basolateral membranes of the cells (unpublished data). The removal of the cleavage site had no influence on the substitution of the core protein with HS-chains (Fig. 2 G) and on the HS-chain charge densities of GPC3 (not depicted). Pulse labeling and chase experiments showed no change in the time course of the endo H-sensitivity of GPC3/AQYA (compare Fig. 2 H with Fig. 1 B). Therefore, the inability of transfected cells to process GPC3/AQYA cannot be attributed to gross impairments of the transport kinetics or trafficking routes followed by the mutant, and we conclude it genuinely reflects the removal of the cleavage site.

Endoproteolytic processing of GPC3 is mediated by PCs

The sequence $R^{355}QYR^{358}$ in GPC3 fits the PC recognition motif (Arg/Lys-$(X)_n$-Arg/Lys, where n = 2, 4, or 6; and X is any amino acid except Cys and rarely Pro). Four members of the PC family, PACE4, PC6, LPC, and furin, have been implicated in the processing of substrates in the constitutive secretory pathway (Taylor et al., 2003). α_1PDX is an engineered mutant of α_1 antitrypsin with an altered active loop, displaying an Arg-X-X-Arg motif that acts specifically as a bait region for intracellular PCs (Creemers et al., 2001). As shown in Fig. 3 A, transient cotransfection with α_1PDX inhibited the processing of both GPC3 (lanes 2 and 4) and GPC3ΔHS, the HS-deficient mutant (lanes 3 and 5). Furin-mediated processing would be consistent with the effect of BFA, A23187, and α_1PDX on GPC3 processing. As a test for the implication of furin itself, we expressed GPC3 in RPE.40 cells, a furin-deficient CHO cell line. RPE.40 cells were unable to process GPC3 (Fig. 3 B, lane 2) unless cotransfected with furin expression vector (Fig. 3 B, lane 4). Substitution of GPC3 with HS, which is acquired in the trans-Golgi compartment, occurred to a similar extent in both CHO-K1 and RPE.40 cells, again implying that the transport and glycosylation of GPC3 are grossly normal in the absence of proteolytic processing. Although these results strongly suggest that furin is involved in GPC3 processing in CHO cells, other members of the PC family might also rescue this processing. Therefore, RPE.40 cells were transfected with GPC3 and a panel of PCs that have broad tissue distributions, including PACE4, PC6 (isoforms A and B), and LPC. Cotransfection with PC6A and PC6B also resulted in cleavage of GPC3 (Fig. 3 C, lanes 3 and 4). The best processing rates were observed for furin, followed by the two isoforms of PC6, whereas PACE4 and LPC cleaved GPC3 only to a limited extent (Fig. 3 C, lanes 2 and 5). In a further experiment, we tested whether furin can directly process GPC3. We treated stably transfected MDCK cells with BFA

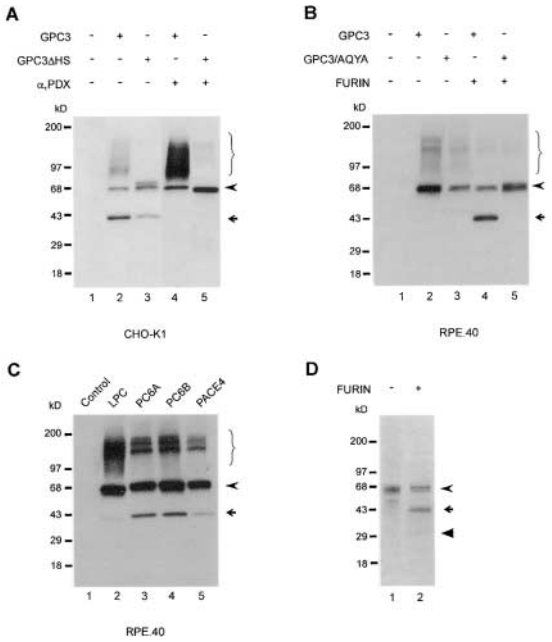

Figure 3. **Identification of PCs as GPC3-processing enzymes.** (A) PC-dependent processing in CHO-K1 cells. CHO-K1 cells were transfected with empty expression vector alone (lane 1), with GPC3 or GPC3ΔHS and empty vector, or with GPC3 or GPC3ΔHS, and with an α_1-PDX expression vector. Total cell extracts were fractionated by SDS-PAGE under reducing conditions and analyzed by Western blotting using anti-HA mAb. (B) Furin-mediated processing in RPE.40 cells. RPE.40 cells were transfected with empty vector, GPC3 or GPC3/AQYA, alone or in combination with a furin expression vector. Western blot analysis of reduced samples using anti-HA antibody. (C) PC-mediated processing in RPE.40 cells. RPE.40 cells were transfected with empty vector only (lane 1) or with GPC3 together with LPC, PC6A, PC6B, and PACE4. Western blot analysis of reduced samples using anti-HA antibody. (D) In vitro digestion of GPC3 with recombinant furin. GPC3 was immunoprecipitated from BFA-treated metabolically labeled transfectant MDCK cells. The immunoprecipitates were mock-digested or digested with recombinant furin, fractionated by SDS-PAGE under reducing conditions, and detected by autoradiography. The curved arrowhead indicates the core protein, the arrow indicates the α-subunit, and the arrowhead indicates the COOH-terminal β subunit. Numbers on the left represent molecular mass markers.

to inhibit the processing, and pulse-labeled these cells for 10 min. After a chase of 60 min, GPC3 was immunopurified from the cell extract and digested in vitro with recombinant furin. Autoradiography revealed that GPC3 was processed in two subunits (Fig. 3 D, lane 2).

GPC3-induced apoptosis depends on processing by PCs and on JNK activation

Some types of cells that are transfected with GPC3 undergo apoptosis. The induction of this apoptosis does not require the HS chains of GPC3 (Gonzalez et al., 1998). To evaluate whether proteolytic processing of GPC3 is necessary, MCF-7 cells were transiently transfected with control vectors GPC3, GPC3/AQYA, or GPC3ΔHS. We confirmed that these constructs were expressed and, except for GPC3/AQYA, processed in these cells (unpublished data). By morphological criteria, a vector control yielded only 2% of apoptotic nuclei. After transfection of GPC3 or GPC3ΔHS,

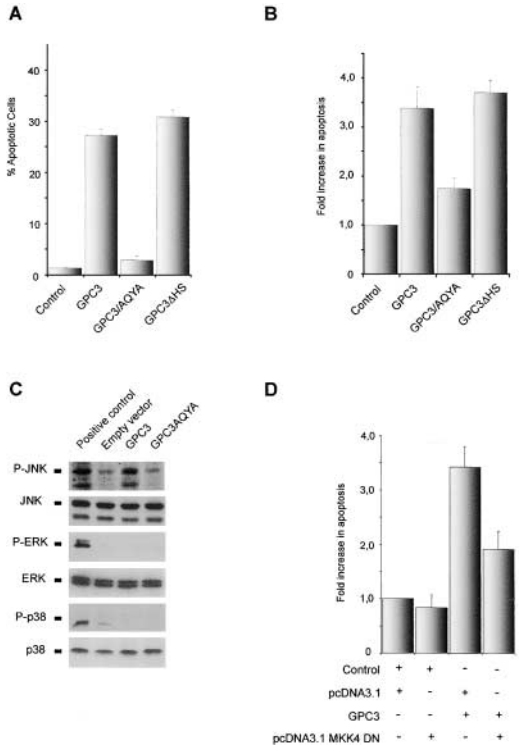

Figure 4. **GPC3-induced apoptosis.** (A and B) Apoptosis depends on GPC3 processing. MCF-7 cells were transiently transfected with a β-galactosidase expression vector and a fivefold excess of control vector, or vectors encoding GPC3, GPC3/AQYA, or GPC3ΔHS. (A) Apoptosis scored by nuclear morphology. The results (mean ± SEM) are shown as a percentage of apoptotic cells (the total number of scored cells taken as 100%). (B) Apoptosis scored by cell death ELISA assay. The results (mean ± SEM) are shown as fold increase in apoptosis, compared with cells transfected with control vector. (C) Processed GPC3 activates JNK. MCF-7 cells were transfected as in A and B. Normalized cell extracts were analyzed by Western blotting, using either anti–phospho-MAPK antibodies or the respective anti-MAPK antibodies. Total cell extracts from UV-treated NIH/3T3 cells were taken as positive control. (D) Apoptosis depends on JNK activation. MCF-7 cells were triple transfected with β-galactosidase expression vector, pcDNA3.1 containing either a dominant-negative MKK4 construct or no insert, and a control vector or a vector encoding GPC3. Apoptosis was measured 48 h after transfection by the cell death ELISA assay, as in B.

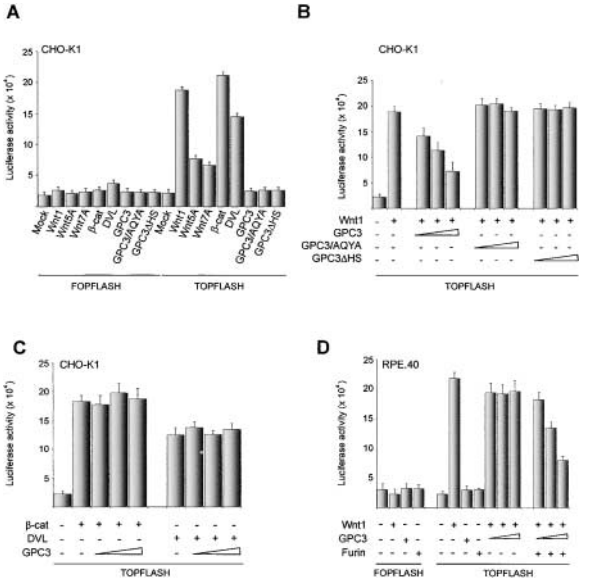

Figure 5. **Processed GPC3 modulates Wnt-initiated canonical signaling.** (A) Activation of β-catenin/TCF-dependent transcription by Wnts and Wnt signal transduction components. CHO-K1 cells were transfected with 0.2 μg of the TOPFLASH or FOPFLASH reporter plasmid, 0.2 μg of β-galactosidase expression vector, and 0.4 μg of the indicated expression plasmids. (B and C) GPC3 overexpression inhibits Wnt signaling, upstream of Dishevelled. CHO-K1 cells were transfected with 0.2 μg of the TOPFLASH reporter plasmid, 0.2 μg of β-galactosidase vector, and 0.4 μg Wnt1, β-cat, or DVL expression vector, along with (from left to right) either 0.2, 0.4, or 0.8 μg of GPC3 or mutant forms of GPC3, as indicated. Empty pDisplay plasmid was added to equalize the total amount of DNA used for transfection. (D) Inhibition of Wnt signaling depends on PC processing. RPE.40 cells were transfected with 0.2 μg of the TOPFLASH or FOPFLASH reporter plasmid, 0.2 μg of β-galactosidase expression vector, and 0.4 μg of furin expression vector, along with varying amounts of GPC3 and empty pDisplay plasmid, as in B and C. Data represent mean ± standard error.

27–30% of the cells displayed typical apoptotic nuclear morphology. In contrast, when transfected with GPC3/AQYA, only 3% of the cells underwent apoptosis (Fig. 4 A). Measuring for the amount of cytoplasmic histone-associated DNA fragments also indicated that GPC3/AQYA was much less effective at inducing apoptosis than wild-type GPC3 or GPC3ΔHS (Fig. 4 B). Thus, lack of processing by convertases nearly abolishes the capacity of the GPC3 protein to induce apoptosis in MCF-7 cells.

Several stimuli that lead to apoptosis activate MAPKs. Looking for potential effectors, we found that GPC3 overexpression in MCF-7 cells results in the phosphorylation of both the 46- and 55-kD isoforms of JNK (Fig. 4 C). There was no effect on ERK or p38. In contrast, overexpression of GPC3/AQYA did not significantly activate any of these kinases. MAPK Kinase 4 (MKK4) is upstream of JNK, and is essential for the full activation of JNK (Davis, 2000). MCF-7 cells cotransfected with dominant-negative MKK4 underwent 42% less apoptosis than cells transfected with only GPC3 (Fig. 4 D), suggesting JNK activation is critical for GPC3-induced apoptosis. Significantly, overexpression of GPC4, tested as an additional control for specificity, did not activate JNK or induce apoptosis in MCF-7 cells (unpublished data).

PC-processed GPC3 modulates Wnt signaling in vitro

GPCs have been implicated in the canonical Wnt signaling pathway, in *D. melanogaster* (Baeg et al., 2001), and in the JNK-dependent convergent extension/planar cell polarity pathway, in zebrafish (Topczewski et al., 2001). Therefore, we examined the effect of GPC3 on Wnt signaling. To test for canonical β-catenin–mediated signaling, we measured the activities of the β-catenin/TCF-responsive reporter pTOPFLASH (Korinek et al., 1997) and the mutant reporter pFOPFLASH. Wnt1, constitutively active β-catenin, DVL-1, and, to a lesser extent, Wnt5A and Wnt7A activated the pTOPFLASH reporter, both in CHO-K1 (Fig. 5 A) and MCF-7 cells (not depicted). By themselves, GPC3, GPC3/AQYA, or GPC3ΔHS did not activate pTOPFLASH (Fig. 5 A). Yet, at invariant levels of Wnt1 in cotransfection mixtures, increasing the amount of wild-type

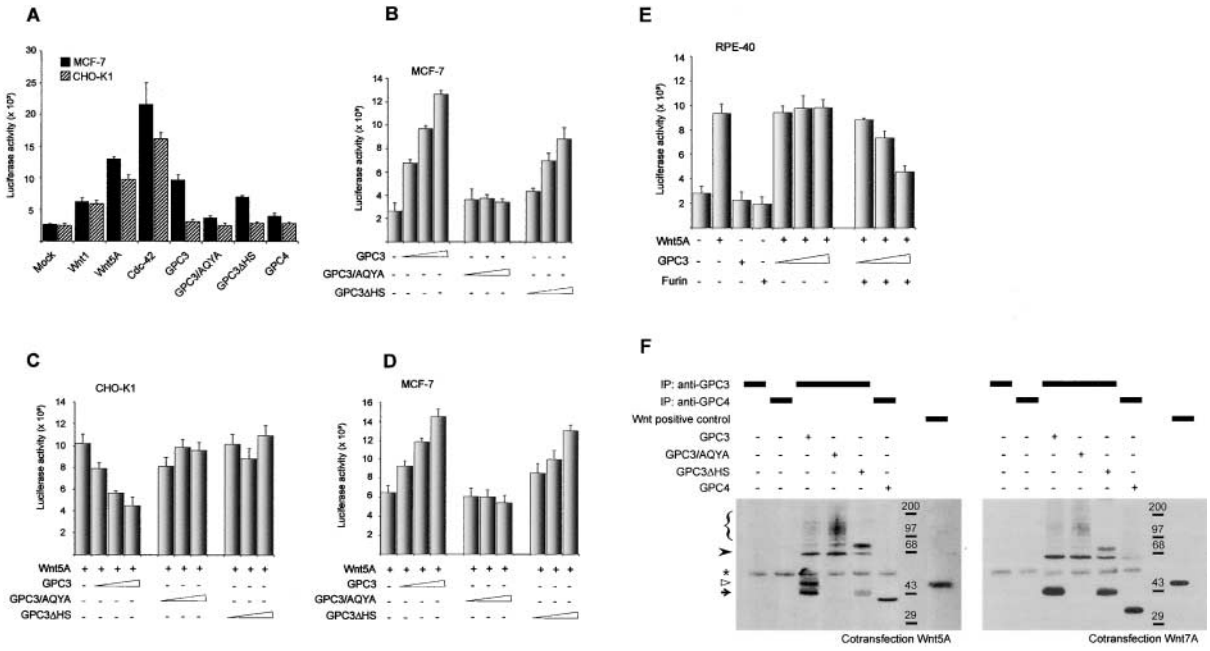

Figure 6. **Processed GPC3 modulates noncanonical Wnt signaling.** (A) Activation of AP-1–dependent transcription by Wnts and GPC3. MCF-7 or CHO-K1 cells were transfected with 0.2 μg of the AP-1–responsive reporter and 0.2 μg of β-galactosidase expression vector, along with 0.4 μg of the indicated expression plasmids. (B) GPC3 dose-dependent activation of AP-1 in MCF-7 cells depends on the processed core protein. MCF-7 cells were transfected with AP-1 reporter plasmid and β-galactosidase (as in A), and (from left to right) 0.2, 0.4, or 0.8 μg of GPC3 or its mutants, as indicated. Empty pDisplay plasmid was added to equalize the total amount of DNA used for transfection. (C and D) GPC3 effects on noncanonical Wnt signaling. CHO-K1 cells or MCF-7 cells were transfected with the AP-1–responsive reporter and β-galactosidase (as in A) and 0.4 μg of Wnt5A expression vector (only 0.2 μg for MCF-7 cells), along with varying amounts of GPC3 or its mutants, and empty pDisplay plasmid (as in B). Wnt inhibition in CHO cells depends on processing and on HS substitution. In MCF-7 cells, processed proteoglycan or core protein further enhances AP-1–dependent transcription. (E) Inhibition of noncanonical Wnt signaling depends on PC processing. RPE.40 cells were transfected with 0.2 μg of the AP-1–responsive reporter, 0.2 μg of β-galactosidase expression vector, 0.4 μg of furin expression plasmid along with varying amounts of GPC3 and empty pDisplay plasmid (as in B). (A–E) Data represent mean ± standard error. (F) Wnt–GPC3 association depends on processing and on HS substitution. MCF-7 cells were cotransfected with HA-tagged Wnt5A or Wnt7A in combination with HA-tagged wild-type GPC3, GPC3/AQYA, GPC3ΔHS, or GPC4. Immunoprecipitates obtained with anti-GPC3/4 polyclonal antibodies were fractionated by SDS-PAGE under reducing conditions, and analyzed by Western blotting, using monoclonal anti-HA antibody. The positive controls are total extracts from Wnt5A/7A-transfected cells. Note that like GPC3, GPC4 is also composed of two disulfide-linked subunits. The upper smear (brace) represents the glycanated form of GPC3. The curved arrowhead indicates the unprocessed core protein, and the arrow indicates the α-subunit. The open arrowhead points to the HA-tagged form of Wnt5A, and the asterisk denotes the IgG heavy chain. Numbers represent molecular mass markers.

GPC3 repressed Wnt1-mediated pTOPFLASH activation in a dose-dependent manner. In contrast, the GPC3/AQYA or the GPC3ΔHS mutant had no effect on Wnt1-induced signaling (Fig. 5 B). Moreover, neither GPC3 (Fig. 5 C), nor GPC3/AQYA (not depicted), nor GPC3ΔHS (not depicted) had any effect on pTOPFLASH reporter activity induced by the overexpression of DVL-1 or constitutively active β-catenin. Together, these results indicate that GPC3 interferes with Wnt/β-catenin signaling upstream of Dishevelled, and suggest that PC processing of the GPC core protein is required for this effect. To confirm this suggestion, pTOPFLASH activity was also measured in furin-deficient CHO cells (RPE.40 cells). As predicted, dose-dependent suppression of canonical Wnt signaling by GPC3 in these cells was dependent on the inclusion of a furin expression construct in the transfections (Fig. 5 D).

To test for effects of GPC3 on the activation of noncanonical Wnt signaling pathways, we monitored the activation of the c-Jun–dependent transcription factor AP-1. Luciferase reporter constructs driven by an AP-1–responsive promotor were strongly activated by dominant-positive Cdc-42 (ninefold increase) and by Wnt5A (fivefold increase), and less efficiently by Wnt1 (twofold increase), both in CHO-K1 cells and in MCF-7 cells (Fig. 6 A). In CHO-K1 cells, where GPC3 does not induce apoptosis, GPC3, GPC3/AQYA or GPC3ΔHS, and also GPC4, by themselves, did not activate the AP-1–luciferase reporter (Fig. 6 A). Importantly, at constant levels of Wnt5A, a potent activator of noncanonical signaling, increasing levels of GPC3 resulted in a dose-dependent decrease in luciferase activity. Increasing concentrations of GPC3/AQYA or GPC3ΔHS had no effect (Fig. 6 C). Together, these results indicate that GPC3 overexpression suppresses noncanonical Wnt signaling in CHO-K1 cells, and suggest that PC processing of the GPC core protein is required also for this effect. This was confirmed by AP-1 reporter assays in RPE.40 cells, where dose-dependent suppression of Wnt5A signaling was dependent on the cotransfection of furin (Fig. 6 E). In contrast, in MCF-7 cells, where GPC3 or GPC3ΔHS expression suffices to stimulate JNK phosphorylation and induce apoptosis (Fig. 4), AP-1–luciferase activity was stimulated by GPC3 (threefold) and GPC3ΔHS (twofold). GPC3/AQYA and

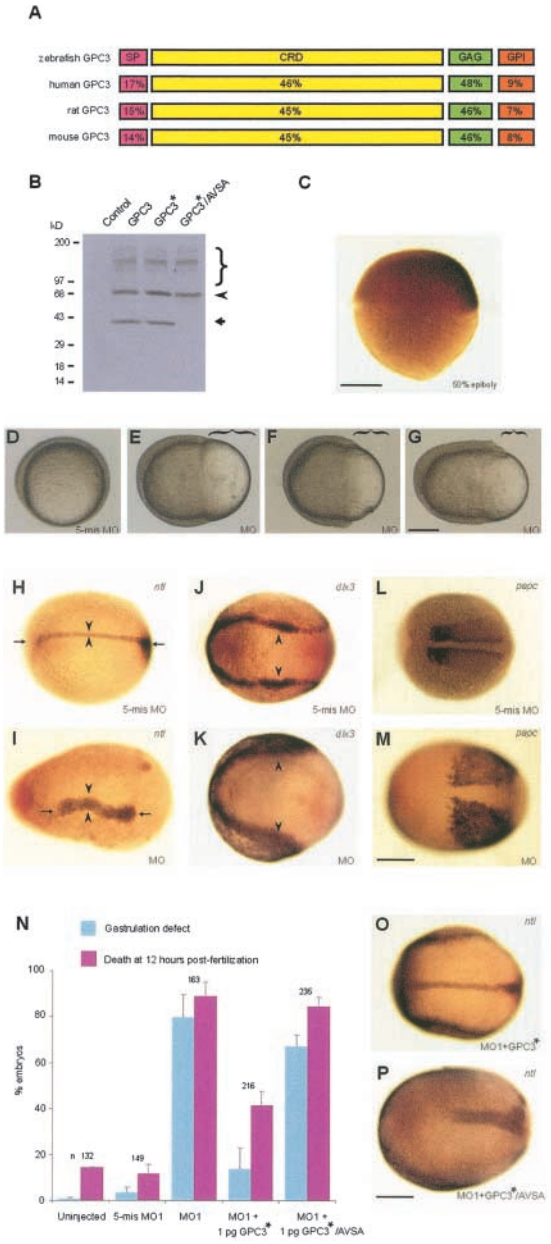

Figure 7. **Interference with GPC3 expression disrupts gastrulation movements in zebrafish.** (A) Predicted domain structure of GPC3 and similarities to GPC3 sequences from other vertebrates. (B) Endoproteolytic processing of the zebrafish GPC3. Whole extracts of CHO-K1 cells transiently transfected with wild-type zebrafish GPC3 or mutant forms, designed not to interact with the morpholinos (GPC3*) and not to be proteolytically processed (GPC3*/AVSA), were analyzed as described in Fig. 2 B. The upper smear (brace) represents the glycanated form of GPC3. The curved arrowhead indicates the unprocessed core protein, and the arrow indicates the α-subunit. Numbers represent molecular mass markers. (C) Expression of *GPC3* at 50% epiboly spreads throughout the animal pole. Detection by in situ hybridization, lateral view with animal pole up. (D–M) Analysis of the *GPC3* morphant phenotype at 10 hpf. (D–G) Lateral views of living embryos injected with control mispair (5-mis MO) and antisense morpholinos (MO). Animal pole is to the left and dorsal is up. Note the arrest of blastoderm movement toward the vegetal pole (brace). (H–M) Dorsal views of control (H, J, and L) and morphant (I, K, and M) embryos. The expressions of three marker genes, indicated at top right, are analyzed by in situ hybridization. Animal pole is to the left. *No tail (ntl)* staining reveals marked shortening (arrows), thickening (curved arrowheads), and undulations of the notochord in the morphants. The shape of the neuroectoderm is outlined by the expression of *distal-less3* (*dlx3*). Note the broadened (curved arrowheads) and shortened neural plate. Widening of *paraxial protocadherin* (*papc*) expression reflects a reduced convergence of presomitic mesoderm. (N–P) Correction of the effects of antisense morpholino MO1 by coinjection of GPC3 mRNA lacking MO-target sequences. Injection of MO1 causes gastrulation defects (less than 80% epiboly at 10 hpf), and the majority of the embryos are dead by 12 hpf. GPC3* mRNA rescues gastrulation and embryo survival (N), and corrects the expression pattern of the *ntl* marker gene (O). GPC3*/AVSA mRNA, encoding a GPC3 protein that cannot be processed, fails to do so (N and P). Results (means and standard errors) of three separate experiments (n, total number of embryos analyzed). Bars, 250 μm.

GPC4, which do not induce apoptosis, had no significant effects on AP-1–luciferase activity (Fig. 6 A). By themselves, GPC3 and GPC3ΔHS, but not GPC3/AQYA, activated the AP-1–responsive reporter in a dose-dependent manner (Fig. 6 B). In further contrast to CHO-K1 cells, increasing the levels of GPC3 or GPC3ΔHS in cotransfections with Wnt5A resulted in a dose-dependent further increase in luciferase activity, but GPC3/AQYA had no effect (Fig. 6 D). Surmising a functional interaction between Wnt5A and processed GPC3, we tested whether in MCF-7 cells, GPC3 might associate with Wnt5A, possibly in a PC-processing–dependent way. Using specific anti-GPC antibodies, we isolated GPCs from MCF-7 cells that were cotransfected with Wnts and GPCs, and probed for the presence of GPCs and Wnts in the immunoprecipitates, using anti-HA antibodies (Fig. 6 F). Wnt5A (but not Wnt7A) coprecipitated with wild-type GPC3, but not with GPC3ΔHS, GPC3/AQYA, or GPC4. These results indicate that, as for the effects of GPC3 on noncanonical signaling in CHO-K1 cells, a stable association between GPC3 and Wnt5A in MCF-7 cells requires both PC processing and substitution with HS, and is specific for GPC3. Altogether, these results identify GPC3 as a regulator of Wnt signaling and indicate that PC processing of the core protein is required for this property.

Interfering with GPC3 processing disrupts gastrulation movements in zebrafish

To establish the relevance of our findings for the in vivo functions of GPC3, we examined the significance of GPC3 and GPC3 processing for early zebrafish development. We identified a cDNA corresponding to zebrafish *GPC3* (GenBank/EMBL/DDBJ accession number AY346090), encoding a protein that is highly similar to GPC3 from other vertebrates, including the characteristic domain structure and a consensus sequence for cleavage by PCs (Fig. 7 A). The HA-tagged wild-type form of zebrafish GPC3 undergoes proteolytic processing in CHO-K1 cells, but zebrafish GPC3/AVSA, a form that is mutant for the $R^{348}VSR^{351}$ PC-cleavage consensus sequence, does not (Fig. 7 B). In situ hybridizations revealed that *GPC3* is maternally expressed and near ubiquitous during blastula and early gastrula stages, but becomes restricted to the prospective hindbrain by 24 hours post fertilization (hpf; Fig. 7 C and not depicted). To investigate the function of GPC3 during zebrafish development, we blocked endogenous *GPC3* expression by the injection of antisense morpholino oligonucleotides (5 ng/embryo). Two

different antisense morpholinos, and their respective 5-mispair controls were tested. The first (MO1) was directed against the exon 2 splice donor site, to block zygotic pre-mRNA splicing. The second (MO2) was targeted to the start codon and 5′ untranslated region, to block GPC3 mRNA translation. Injection of MO1 or MO2 caused severe defects during epiboly, an early movement that drives cells toward the vegetal pole to cover the entire yolk by the end of gastrulation. While the blastoderm was spread over the entire yolk in control-injected embryos (100% epiboly), at 10 hpf most of the MO-injected embryos were arrested at 60–80% epiboly (Fig. 7, D–G). The majority of these embryos died a few hours later (Fig. 7 N).

Tracing the expression of several marker genes further documented morphogenetic abnormalities. The expression domain of *ntl* in the chordamesoderm was shortened and widened in MO-injected embryos (Fig. 7, H and I). The expression domain of *dlx3*, marking the boundaries of the neuroectoderm, revealed a mediolateral broadening of the neural plate during early segmentation (Fig. 7, J and K). Widening of the *papc* expression reflected reduced convergence of presomitic mesoderm (Fig. 7, L and M). These results indicate that *GPC3* plays essential roles during gastrulation by affecting cell movements without significantly contributing to early cell fate specification. None of the 5-mispair control morpholinos had such effects. The specificity of the MO effects was further documented by "rescue" experiments. Whereas ∼80% of the MO-injected embryos exhibited gastrulation defects, coinjection of 1 pg RNA encoding full-length HA-tagged zebrafish GPC3, so designed to not interact with the morpholinos, significantly reduced this figure to ∼15% (Fig. 7 N). To evaluate the importance of GPC3 processing for function, we coinjected 1 pg of RNA encoding GPC3/AVSA mutant protein. Unlike wild-type GPC3 (Fig. 7, N and O), this mutant did not rescue embryo morphogenesis or survival (Fig. 7, N and P). These results indicate that loss of GPC3 function affects cell movements during gastrulation, and that abolishing the proteolytic processing of GPC3 blocks normal GPC3 function.

Discussion

HS is strongly implicated in the control of normal cell growth and development, regulating events ranging from branching morphogenesis to left–right patterning (Lander and Selleck, 2000). Most explored in the context of development is its contribution to FGF and Wnt signaling. In GPCs, this versatile HS is linked to highly conserved proteins with complex structures, but with no known functions other than controlling the display of HS at the cell surface. Genetic evidence has identified GPCs as mediators of the canonical Wg signaling pathway in *D. melanogaster* (Tsuda et al., 1999; Baeg et al., 2001), and as mediators of the "Wnt–polarity" pathway that regulates movements of convergent extension in *X. laevis* and zebrafish (Topczewski et al., 2001; Ohkawara et al., 2003). In this paper, we identify an endoproteolytic processing of the GPC3 core protein. This processing is mediated by PCs and is necessary for the modulation of Wnt signaling, for cell type-specific negative effects on cell survival that implicate JNK activation, and for the regulation of gastrulation movements in zebrafish.

GPC3 clearly influences both canonical and noncanonical Wnt signaling in vitro. It acts upstream of Dishevelled, and can be recovered in physical association with Wnts, which would be consistent with a role in ligand reception, capturing the ligands and controlling their availability for interaction with cognate receptors that transduce the signal. The processed core protein is essential, but not sufficient, for this activity, as modulation of Wnt signaling and physical association with Wnt do not occur unless the processed protein is substituted with HS. It has already been pointed out that the CRD of the GPCs bears some structural resemblance to the CRD of the Frizzled Wnt receptors (Topczewski et al., 2001). The PC cleavage site occurs just downstream of this region of homology. Therefore, one possible scheme could be that the processing facilitates the interaction of the Frz motif in the CRD with one or several members of the Wnt family. In that case, the data would suggest that the intrinsic affinity of the exposed protein-binding site is too weak, and that binding needs the Wnt ligand also to be bound to an HS chain that forms part of the proteoglycan, the chain and the protein acting as the two stems of molecular tweezers that withhold the ligand.

Although GPC3 inhibits Wnt signaling in our cellular bioassays, it is not clear whether overexpressions represent physiological assessments of function. Wnts are important regulators of cell growth and survival, and there seems to be an important role for inhibition of Wnt signaling in response to different stress signals that all converge on the activation of c-Jun and apoptosis in vivo (Grotewold and Ruther, 2002). In some cells or cellular contexts, one possible consequence of an overabundance of GPC3 tweezers could be that they withdraw Wnts from antiapoptotic signaling cascades. Yet, although excess Wnt or downstream Wnt signal transduction components are counterbalancing the apoptosis of MCF-7 cells (unpublished data), this scheme is not a sufficient explanation for the apoptosis that is initiated by GPC3 in these cells. Indeed, unlike in the inhibition of Wnt signaling, a bare, unsubstituted core protein suffices for inducing this apoptosis, provided it is processed by PCs. Therefore, we propose that processing also exposes a GPC3 core protein determinant that interacts directly, and without assistance of any HS, with another, as yet unidentified cell-specific component, and that in appropriate contexts the formation of this complex initiates a signaling cascade that converges on JNK activation and apoptosis. Proposing that the processed core protein of GPC3 also impinges on signaling paths other than those activated by Wnts would be consistent with the genetic evidence that identifies Dally and GPC3 as enhancers of Dpp/Bmp4 signaling (Jackson et al., 1997; Tsuda et al., 1999; Paine-Saunders et al., 2000; Grisaru et al., 2001; Fujise et al., 2003).

Functional and genetic studies in *D. melanogaster* have implicated JNK as a component of the Wnt–polarity pathway. More recently, it was shown that JNK also plays a role in regulating convergent extension movements during gastrulation in vertebrate embryos (Yamanaka et al., 2002). GPC3, which can modulate pathways that control the activation of JNK, appears important for the control of gastrulation movements

in zebrafish. The GPC3 morphant phenotype, with mispositioning of the expressions of the mesendoderm/neuroectoderm-specific genes *ntl*, *papc*, and *dlx3*, resembles the phenotypes of embryos with loss-of-function mutations in *wnt11/silberblick*, *wnt5A/pipetail*, and *GPC4/knypek* (Rauch et al., 1997; Heisenberg et al., 2000; Topczewski et al., 2001). Therefore, the data would fit the idea that GPC3 is required for receiving Wnt5A or Wnt11 signals and activating noncanonical Wnt pathways leading to JNK, similar to the role of *knypek* in convergence/extension. However, unlike *knypek/GPC4, GPC3* also has an effect on epiboly, suggesting nonoverlapping functions for the various GPCs. Future experiments, addressing genetic interactions with Wnts, should clarify the validity of this proposal.

Patients with loss-of-function mutations of *GPC3* and *Gpc3*-deficient mice show generalized overgrowth, and some of the clinical manifestations of the SGBS (e.g., syndactyly and supernumerary nipples) strongly suggest locally defective apoptotic signaling programs. Patients with SGBS often develop embryonal tumors (neuroblastoma and Wilms' tumor), and loss of GPC3 expression has been reported in several tumors (Lin et al., 1999; Xiang et al., 2001). Inhibition of Wnt signals that are involved in cell proliferation and cell survival, and direct effects on apoptotic signaling cascades, could be physiological roles of GPC3; this is consistent with the in vitro data that help explain these phenotypes and the implication of GPC3 as a potential tumor suppressor. Because these roles depend on PC processing, failure or absence of processing may explain possible expression paradoxes (Midorikawa et al., 2003). Fitting GPC3 in signaling pathways will have to consider that its loss or overexpression might represent the loss or gain of an HS moiety that potentially impinges on many ligands and pathways, and of a unique protein that may be dedicated to more unique functions. The expressions of the various GPCs show substantial overlap (Veugelers et al., 2000). In case of loss, compensating HSPG expressions may easily rescue the HS deficit, whereas rescue of the dedicated function may critically depend on the nature of the protein core, which does or does not share this function with GPC3, and, possibly, its relationship as substrate to proprotein-converting enzymes in the tissues. In this context, we have preliminary evidence that GPC4, which does not induce apoptosis in MCF-7 cells, is processed by PCs in MCF-7 and other cells. In contrast, GPC5, the GPC that is most closely related to GPC3, is not processed and also does not induce apoptosis in these cells (unpublished data). Inspection of the sequences of the various GPCs indicates that they all contain potential PC-cleavage sites at corresponding levels in their CRDs; currently, we are exploring whether unique GPC–PC substrate–enzyme relationships might exist. Indeed, the members of the PC family display similar, but not identical, specificity for basic motifs at the cleavage site of their substrates. Processing may also be regulated. With respect to Dally, there is no conclusive evidence explaining how Dally affects Wg signaling in some tissues and Dpp in others. Whereas tissue-specific differences in HS structure were proposed, perhaps tissue-specific differences in PC-mediated processing have to be considered as one additional possibility.

Our current experiments aim at addressing these various issues, but the data in the present paper strongly argue that endoproteolytic processing of the GPC core proteins by PCs is essential for their signaling activities.

Materials and methods

Plasmid constructs

All cDNAs were introduced into pDisplay or pcDNA (Invitrogen). The HA-tagged GPC3 construct has been described previously (Veugelers et al., 2000). QuickChange (Stratagene) was used to modify GPC3. In all cases, mutagenesis was confirmed by sequencing. PC expression vectors were described previously (Creemers et al., 2001). The α_1PDX-cDNA was provided by G. Thomas (Oregon Health Sciences University, Portland, OR) and dominant-negative MKK4 was a gift of P. Agostinis (University of Leuven, Leuven, Belgium). Wnt expression vectors were provided by J. Kitajewski (Columbia University, New York, NY). The DVL-1 and DVL-1 deletion mutants were provided by P. Salinas (Imperial College of Science, London, UK). The ΔN90 stabilized β-catenin construct was obtained from S. Tejpar (University of Leuven, Leuven, Belgium). The pTOPFLASH and pFOPFLASH reporter constructs were gifts of H. Clevers (Hubrecht Laboratory, Utrecht, Netherlands). The AP-1 reporter construct was provided by M. Baens (University of Leuven, Leuven, Belgium). The activated form of Cdc42 was obtained from A. Hall (University College, London, UK).

Cell culture and transfections

Cells were routinely grown in 6-well plates, in DME/F12 supplemented with 10% FBS (Hyclone). MDCK cells were transfected by electroporation, and stable transfectants were selected as described previously (Mertens et al., 1996). COS-1, CHO-K1, and RPE.40 cells were transfected using LipofectAMINE PLUS (Invitrogen). Transient transfection assays in MCF-7 cells were conducted as described by Gonzalez et al. (1998).

Apoptosis assays

Cells were transfected with β-galactosidase expression vector (Promega) and a fivefold excess of pDisplay vector, without insert or encoding wild-type or mutant GPC3. The serum was removed 12 h after transfection, and apoptosis was scored 36 h after serum withdrawal. Cells grown on glass coverslips were fixed in 4% PFA for 30 min, stained with DAPI (Sigma-Aldrich), and examined by fluorescence microscopy. Apoptotic nuclei were counted in at least 10 fields, with a minimum of 100 cells per field. Cells grown in 6-well plates were scored by cell death ELISA assay (Roche).

Detection of MAPKs

The medium was removed 12 h after transfection, and the cells were further grown for 12 h in DME/F12 supplemented with 1% FBS. Cells were washed, and lysed in ice-cold homogenization buffer (50 mM β-glycerophosphate, pH 7.3, 1.5 mM EGTA, 1.0 mM EDTA, 0.1 mM sodium vanadate, 1.0 mM benzamidine, 10 μg/ml aprotinin, 10 μg/ml leupeptin, 2.0 μg/ml pepstatin A, and 10 mM DTT) containing 1% Triton X-100. Cleared cell lysates, normalized for β-galactosidase activity, were fractionated by electrophoresis in 10% SDS-PAGE (Bio-Rad Laboratories) and transferred to Hybond C-extra membranes (Amersham Biosciences). The membranes were probed with mouse anti–phospho-ERK1/2, rabbit anti–phospho-p38, rabbit anti-p38 (New England Biolabs, Inc.), rabbit anti-JNK, rabbit anti–phospho-JNK (Upstate Biotechnology), and rabbit anti-ERK1/2 (Sigma-Aldrich) diluted in blocking buffer (TBS; 0.1% Tween-20 and 5% nonfat dry skim milk). Bound antibody was detected with species-specific secondary antiserum conjugated with peroxidase, using an ECL detection system (Amersham Biosciences).

Proteoglycan extraction and detection

Extraction buffers containing Triton X-100 or octylglucoside, and procedures used to isolate the proteoglycans from cell extracts or media fractions were performed as described previously (Lories et al., 1989). Samples (normalized for number of cells) were fractionated by SDS-PAGE under reducing or nonreducing conditions and transferred to cationic nylon membranes (Bio-Rad Laboratories). HA-tagged proteins were detected with the rat mAb 3F10 (Roche). Binding of primary antibody was detected with goat anti–rat secondary antibody conjugated to alkaline phosphatase (Calbiochem), the chemiluminescent substrate CSPD, and Nitro-Block-II™ Luminescence Enhancer (Applied Biosystems).

Metabolic labeling and immunoprecipitation

After a preincubation in methionine- and cysteine-free DME supplemented with 0.1% BSA (Sigma-Aldrich) for 30 min at 37°C, cells were labeled for

10 min in similar medium containing 100 μCi/ml of [^{35}S]cysteine-methionine (ICN Biomedicals), followed by a chase in DME/F12 supplemented with 10% FCS for the times indicated. Cells were lysed in OG extraction buffer. Cleared cell lysates were preabsorbed with protein A–Sepharose (Amersham Biosciences) for 30 min at 4°C, and then incubated with 10 μg of the mouse anti-HA mAb (12CA5; Roche) coupled to protein A–Sepharose for 3 h at 4°C. The beads were washed with OG extraction buffer, and bound material was eluted by boiling in 1% SDS for 5 min.

Enzyme treatments

Proteoglycan extracts were dialyzed against enzyme buffer and digested with chondroitinase ABC or heparitinase (Seikagaku) as described previously (Lories et al., 1989). Digested immunoprecipitates were aliquoted and treated with endoglycosidase H (Roche) or furin (Affinity BioReagents, Inc.) as recommended by the manufacturers.

Confocal laser scanning microscopy

Stable MDCK clones were fixed with 4% PFA in 0.1 M phosphate buffer for 30 min at 25°C. Where indicated, the cells were permeabilized with 0.1% Triton X-100. After blocking, the cells were incubated with rat anti-HA mAb 3F10 for 2 h at 25°C. Binding of primary antibody was detected with Alexa 594–conjugated anti–rat IgG (Molecular Probes) by confocal laser scanning microscopy (model MRC 1024; Bio-Rad Laboratories).

Luciferase assays for TOP/FOPFLASH and AP-1 reporter activities

MCF-7 or CHO-K1 cells were transiently transfected with a combination of plasmids as described the legends to Figs. 5 and 6. Cells were lysed 24 h after transfection. Luciferase (Promega) and β-galactosidase (Applied Biosystems) assays were performed as specified by the manufacturers. For each experiment, the transfections were performed in triplicate. The results are represented as the means ± SD of at least three independent experiments (nine separate transfections). All values were normalized for transfection efficiency (β-galactosidase activity).

Wnt-GPC coimmunoprecipitation experiments

Synthetic peptides (corresponding to the amino acid residues 50–65 of GPC3 and 67–82 of GPC4) were used to raise and isolate affinity-purified GPC-specific rabbit polyclonal antibodies (Eurogentec). OG extracts of transfected MCF-7 cells were cleared and preabsorbed as described in Metabolic labeling and immunoprecipitation, and mixed overnight with a fresh sample of protein A-Sepharose and 10 μg of anti-GPC3 or anti-GPC4.

Approaches in zebrafish

Zebrafish were kept and bred according to standard protocols (Westerfield, 1995). The zebrafish GPC3 EST clone (ICRFp524K17141Q8) was purchased from RZPD. GPC3 constructs for RNA injection were generated by PCR and cloned into pCS2+. Capped mRNA was synthesized in vitro from linearized plasmids, using the mMESSAGE mMACHINE SP6 kit (Ambion). FITC-conjugated antisense morpholinos with the sequences 5′-TAGCAGAAACTCACCTTGAAAGAGG-FITC-3′ (MO1) and 5′-ATAAGGCTTCCAGATGACAGGTTTG-FITC-3′ (MO2), and the respective FITC-conjugated 5-mispair antisense control morpholinos (5-mis MO) were obtained from Gene Tools, LLC. RNA and/or antisense morpholinos were injected into one- or two-cell stage embryos. Embryos with a homogenous fluorescence were collected at 4 hpf and scored when controls reached bud stage (10 hpf). Embryos reaching < 80% epiboly by that time were scored as "gastrulation-defective." Whole-mount in situ hybridization was performed as described by Jowett (2001), using the indicated probes.

B. De Cat is the recipient of a fellowship from the Vlaams Instituut voor de bevordering van het Wetenschappelijk – Technologisch onderzoek in de Industrie. This work has been supported by grants from the Fonds voor Wetenschappelijk Onderzoek-Vlaanderen, the Research Fund K.U. Leuven, the Interuniversity Attraction Poles, and the Flanders Interuniversity Institute for Biotechnology.

Submitted: 24 February 2003
Accepted: 16 September 2003

References

Baeg, G.H., X. Lin, N. Khare, S. Baumgartner, and N. Perrimon. 2001. Heparan sulfate proteoglycans are critical for the organization of the extracellular distribution of Wingless. *Development.* 128:87–94.

Cano-Gauci, D.F., H.H. Song, H. Yang, C. McKerlie, B. Choo, W. Shi, R. Pullano, T.D. Piscione, S. Grisaru, S. Soon, et al. 1999. Glypican-3–deficient mice exhibit developmental overgrowth and some of the abnormalities typical of Simpson–Golabi–Behmel syndrome. *J. Cell Biol.* 146:255–264.

Chen, R.L., and A.D. Lander. 2001. Mechanisms underlying preferential assembly of heparan sulfate on glypican-1. *J. Biol. Chem.* 276:7507–7517.

Chiao, E., P. Fisher, L. Crisponi, M. Deiana, I. Dragatsis, D. Schlessinger, G. Pilia, and A. Efstratiadis. 2002. Overgrowth of a mouse model of the Simpson–Golabi–Behmel syndrome is independent of IGF signaling. *Dev. Biol.* 243: 185–206.

Creemers, J.W., D. Ines Dominguez, E. Plets, L. Serneels, N.A. Taylor, G. Multhaup, K. Craessaerts, W. Annaert, and B. De Strooper. 2001. Processing of beta-secretase by furin and other members of the proprotein convertase family. *J. Biol. Chem.* 276:4211–4217.

Davis, R.J. 2000. Signal transduction by the JNK group of MAP kinases. *Cell.* 103: 239–252.

Fujise, M., S. Takeo, K. Kamimura, T. Matsuo, T. Aigaki, S. Izumi, and H. Nakato. 2003. Dally regulates Dpp morphogen gradient formation in the *Drosophila* wing. *Development.* 130:1515–1522.

Gonzalez, A.D., M. Kaya, W. Shi, H. Song, J.R. Testa, L.Z. Penn, and J. Filmus. 1998. OCI-5/GPC3, a glypican encoded by a gene that is mutated in the Simpson–Golabi–Behmel overgrowth syndrome, induces apoptosis in a cell line–specific manner. *J. Cell Biol.* 141:1407–1414.

Grisaru, S., D. Cano-Gauci, J. Tee, J. Filmus, and N.D. Rosenblum. 2001. Glypican-3 modulates BMP- and FGF-mediated effects during renal branching morphogenesis. *Dev. Biol.* 231:31–46.

Grotewold, L., and U. Ruther. 2002. The Wnt antagonist Dickkopf-1 is regulated by Bmp signaling and c-Jun and modulates programmed cell death. *EMBO J.* 21:966–975.

Heisenberg, C.P., M. Tada, G.J. Rauch, L. Saude, M.L. Concha, R. Geisler, D.L. Stemple, J.C. Smith, and S.W. Wilson. 2000. Silberblick/Wnt11 mediates convergent extension movements during zebrafish gastrulation. *Nature.* 405: 76–81.

Jackson, S.M., H. Nakato, M. Sugiura, A. Jannuzi, R. Oakes, V. Kaluza, C. Golden, and S.B. Selleck. 1997. Dally, a *Drosophila* glypican, controls cellular responses to the TGF-beta-related morphogen, Dpp. *Development.* 124: 4113–4120.

Jowett, T. 2001. Double in situ hybridization techniques in zebrafish. *Methods Enzymol.* 23:345–358.

Korinek, V., N. Barker, P.J. Morin, D. van Wichen, R. de Weger, K.W. Kinzler, B. Vogelstein, and H. Clevers. 1997. Constitutive transcriptional activation by a beta-catenin-Tcf complex in APC−/− colon carcinoma. *Science.* 275: 1784–1787.

Lander, A.D., and S.B. Selleck. 2000. The elusive functions of proteoglycans: in vivo veritas. *J. Cell Biol.* 148:227–232.

Lin, H., R. Huber, D. Schlessinger, and P.J. Morin. 1999. Frequent silencing of the GPC3 gene in ovarian cancer cell lines. *Cancer Res.* 59:807–810.

Lories, V., J.J. Cassiman, H. Van den Berghe, and G. David. 1989. Multiple distinct membrane heparan sulfate proteoglycans in human lung fibroblasts. *J. Biol. Chem.* 264:7009–7016.

Mertens, G., B. Van der Schueren, H. van den Berghe, and G. David. 1996. Heparan sulfate expression in polarized epithelial cells: the apical sorting of glypican (GPI-anchored proteoglycan) is inversely related to its heparan sulfate content. *J. Cell Biol.* 132:487–497.

Midorikawa, Y., S. Ishikawa, H. Iwanari, T. Imamura, H. Sakamoto, K. Miyazono, T. Kodama, M. Makuuchi, and H. Aburatani. 2003. Glypican-3, overexpressed in hepatocellular carcinoma, modulates FGF2 and BMP-7 signaling. *Int. J. Cancer.* 103:455–465.

Ohkawara, B., T.S. Yamamoto, M. Tada, and N. Ueno. 2003. Role of glypican 4 in the regulation of convergent extension movements during gastrulation in Xenopus laevis. *Development.* 130:2129–2138.

Paine-Saunders, S., B.L. Viviano, J. Zupicich, W.C. Skarnes, and S. Saunders. 2000. Glypican-3 controls cellular responses to Bmp4 in limb patterning and skeletal development. *Dev. Biol.* 225:179–187.

Pilia, G., R.M. Hughes-Benzie, A. MacKenzie, P. Baybayan, E.Y. Chen, R. Huber, G. Neri, A. Cao, A. Forabosco, and D. Schlessinger. 1996. Mutations in GPC3, a glypican gene, cause the Simpson-Golabi-Behmel overgrowth syndrome. *Nat. Genet.* 12:241–247.

Rauch, G.J., M. Hammerschmidt, P. Blader, H.E. Schauerte, U. Strahle, P.W. Ingham, A.P. McMahon, and P. Haffter. 1997. Wnt5 is required for tail formation in the zebrafish embryo. *Cold Spring Harb. Symp. Quant. Biol.* 62:

227–234.

Song, H.H., and J. Filmus. 2002. The role of glypicans in mammalian development. *Biochim. Biophys. Acta.* 1573:241–246.

Taylor, N.A., W.J.M. Van De Ven, and J.W.M. Creemers. 2003. Curbing activation: proprotein convertases in homeostasis and pathology. *FASEB J.* 17: 1215–1227.

Topczewski, J., D.S. Sepich, D.C. Myers, C. Walker, A. Amores, Z. Lele, M. Hammerschmidt, J. Postlethwait, and L. Solnica-Krezel. 2001. The zebrafish glypican knypek controls cell polarity during gastrulation movements of convergent extension. *Dev. Cell.* 1:251–264.

Tsuda, M., K. Kamimura, H. Nakato, M. Archer, W. Staatz, B. Fox, M. Humphrey, S. Olson, T. Futch, V. Kaluza, et al. 1999. The cell-surface proteoglycan Dally regulates Wingless signalling in *Drosophila*. *Nature.* 400:276–280.

Tsuda, M., S. Izumi, and H. Nakato. 2001. Transcriptional and posttranscriptional regulation of the gene for Dally, a *Drosophila* integral membrane proteoglycan. *FEBS Lett.* 494:241–245.

Veugelers, M., B.D. Cat, S.Y. Muyldermans, G. Reekmans, N. Delande, S. Frints, E. Legius, J.P. Fryns, C. Schrander-Stumpel, B. Weidle, et al. 2000. Mutational analysis of the GPC3/GPC4 glypican gene cluster on Xq26 in patients with Simpson-Golabi-Behmel syndrome: identification of loss-of-function mutations in the GPC3 gene. *Hum. Mol. Genet.* 9:1321–1328.

Westerfield, M. 1995. The Zebrafish Book. A Guide for the Laboratory Use of Zebrafish (*Danio Rerio*). University of Oregon Press, Eugene, OR. 307 pp.

Xiang, Y.Y., V. Ladeda, and J. Filmus. 2001. Glypican-3 expression is silenced in human breast cancer. *Oncogene.* 20:7408–7412.

Yamanaka, H., T. Moriguchi, N. Masuyama, M. Kusakabe, H. Hanafusa, R. Takada, S. Takada, and E. Nishida. 2002. JNK functions in the non-canonical Wnt pathway to regulate convergent extension movements in vertebrates. *EMBO Rep.* 3:69–75.